Nup132 modulates meiotic spindle attachment in fission yeast by regulating kinetochore assembly

Hui-Ju Yang,[1] Haruhiko Asakawa,[1] Tokuko Haraguchi,[1,2] and Yasushi Hiraoka[1,2]

[1]Graduate School of Frontier Biosciences, Osaka University, Suita 565-0871, Japan
[2]Advanced ICT Research Institute Kobe, National Institute of Information and Communications Technology, Iwaoka-cho, Nishi-ku, Kobe 651-2492, Japan

During meiosis, the kinetochore undergoes substantial reorganization to establish monopolar spindle attachment. In the fission yeast *Schizosaccharomyces pombe*, the KNL1–Spc7-Mis12-Nuf2 (KMN) complex, which constitutes the outer kinetochore, is disassembled during meiotic prophase and is reassembled before meiosis I. Here, we show that the nucleoporin Nup132 is required for timely assembly of the KMN proteins: In the absence of Nup132, Mis12 and Spc7 are precociously assembled at the centromeres during meiotic prophase. In contrast, Nuf2 shows timely dissociation and reappearance at the meiotic centromeres. We further demonstrate that depletion of Nup132 activates the spindle assembly checkpoint in meiosis I, possibly because of the increased incidence of erroneous spindle attachment at sister chromatids. These results suggest that precocious assembly of the kinetochores leads to the meiosis I defects observed in the *nup132*-disrupted mutant. Thus, we propose that Nup132 plays an important role in establishing monopolar spindle attachment at meiosis I through outer kinetochore reorganization at meiotic prophase.

Introduction

Meiosis is an important process for sexually reproducing eukaryotes and generates inheritable haploid gametes from a parental diploid cell. Through meiosis, genome ploidy is halved via two consecutive rounds of chromosome segregation after a single round of DNA replication. The first meiotic division is an uncommon chromosome segregation step in which homologous chromosomes are segregated but sister chromatids remain attached. To maintain the attachment between sister chromatids during meiosis I, the sister centromeres are rearranged into a meiosis-specific mono-oriented structure so that the sister centromeres are attached to microtubules that originate from the same poles (monopolar spindle attachment; Hauf and Watanabe, 2004; Parra et al., 2004). In contrast, the second meiotic division, like mitosis, segregates sister chromatids. In meiosis II, the sister centromeres bind to microtubules that are derived from opposite spindle poles (bipolar spindle attachment). Understanding the mechanisms underlying faithful segregation of chromosomes is clinically important because chromosome missegregation during meiosis is a major cause of human miscarriage and trisomy disorders.

Studies in the fission yeast *Schizosaccharomyces pombe* have revealed that establishment of the mono-oriented centromere in meiosis I requires the meiosis-specific cohesin Rec8 and that monopolar spindle attachment is supported by chiasmata formed between the homologous chromosomes (Watanabe and Nurse, 1999; Molnar et al., 2001a,b; Yamamoto and Hiraoka, 2003; Hirose et al., 2011). During meiotic prophase, Rec8 holds sister chromatids together along the chromosome arms and centromeric regions (Watanabe and Nurse, 1999; Ding et al., 2006). Homologous chromosome recombination that is initiated by programmed meiotic double-strand breaks (DSBs) results in chiasma formation and physically connects the two homologues. In cooperation with the meiosis-specific centromere protein Moa1, Rec8 mono-orients the sister centromeres (Watanabe and Nurse, 1999; Yokobayashi and Watanabe, 2005). The pulling force that the spindles exert on the mono-oriented sister centromeres is stabilized by the tension generated via chiasmata formation between the homologues (Hauf and Watanabe, 2004; Parra et al., 2004; Hirose et al., 2011). Once the tension is sensed, cohesion of the chromosome arms is lost because of separase cleavage of Rec8, which allows homologous chromosome separation (Watanabe and Nurse, 1999; Molnar et al., 2001a,b; Kitajima et al., 2003; Yamamoto and Hiraoka, 2003; Hirose et al., 2011). *S. pombe* shugoshin (Sgo1) protects centromeric Rec8 from cleavage, which keeps the sister chromatids together at anaphase I (Watanabe and Nurse, 1999; Kitajima et al., 2004; Ding et al., 2006). In the *rec8*Δ and recombination mutants, the frequency of untimely sister chromatid segregation in meiosis I is increased (Watanabe and Nurse, 1999; Molnar et al., 2001a; Yamamoto and Hiraoka, 2003; Yokobayashi and Watanabe, 2005). When the tension at the centromeres is lost, such as in the achiasmate *rec12* mutant,

Correspondence to Yasushi Hiraoka: hiraoka@fbs.osaka-u.ac.jp

Abbreviations used in this paper: APC, anaphase-promoting complex; DSB, double-strand break; KMN, KNL1–Spc7-Mis12-Nuf2; ME, malt extract; SAC, spindle assembly checkpoint; Sgo1, *S. pombe* shugoshin; SPB, spindle pole body; YES, yeast extract with supplements.

The Rockefeller University Press $30.00
J. Cell Biol. Vol. 211 No. 2 295–308
www.jcb.org/cgi/doi/10.1083/jcb.201501035

the spindle assembly checkpoint (SAC) is activated, which halts cells in metaphase I (Yamamoto et al., 2008). Components of the SAC are localized to the centromeres during metaphase and function as a surveillance system to ensure that the centromeres are attached to the microtubules under the appropriate tension (Uchida et al., 2009). Activation of the SAC inhibits the activity of the anaphase-promoting complex (APC) to prevent anaphase from proceeding until the tension at the centromeres is generated (Kitajima et al., 2003).

The kinetochore at the centromere plays an important role in microtubule attachment. In addition to Rec8-mediated mono-orientation of centromeres, reorganization of the outer kinetochore components, known as the KNL1–Spc7-Mis12-Nuf2 (KMN) proteins, is also thought to assist in monopolar spindle attachment to the centromeres at meiosis I (Asakawa et al., 2005; Hayashi et al., 2006). The KMN complex functions as a molecular mechanical sensor that monitors microtubule-kinetochore attachment (Rago and Cheeseman, 2013). The KNL1/Spc7 family proteins are required for recruiting the SAC components as well as the factors that activate or deactivate SAC (Desai et al., 2003; Espeut et al., 2012; Shepperd et al., 2012). The Nuf2 complex binds directly to microtubules (Cheeseman et al., 2006), and the Mis12 complex links the Nuf2 complex to the inner kinetochores (Przewloka et al., 2011; Screpanti et al., 2011). The stable association between the Nuf2 complex and microtubules silences SAC activity. Although the KMN proteins are constitutive components of the outer kinetochores throughout the mitotic cell cycle, they transiently dissociate from the meiotic kinetochores during meiotic prophase in *S. pombe* (Hayashi et al., 2006). During the mitotic cell cycle, the centromeres cluster at the spindle pole body (SPB; a centrosome-equivalent structure in yeast), whereas the telomeres are located away from the SPB (Hou et al., 2012). In contrast, during meiotic prophase, the telomeres are brought to the SPB (Chikashige et al., 1994, 2006). At the same time, the centromeres detach from the SPB because of disassembly of the KMN proteins from the centromeres (Chikashige et al., 1997; Asakawa et al., 2005; Hayashi et al., 2006). Interestingly, when mating pheromone is absent, the KMN proteins persist and localize at the centromeres during meiotic prophase, and precocious sister chromatid segregation at meiosis I is often observed (Yamamoto and Hiraoka, 2003; Chikashige et al., 2004; Asakawa et al., 2005; Hayashi et al., 2006). This observation suggested that mating pheromone signaling, probably through transient dissociation of the KMN proteins, promotes kinetochore reorganization in favor of monopolar spindle attachment of sister chromatids. However, loading of the Rec8 protector Sgo1 onto the centromeres is also mating pheromone-signaling dependent (Hayashi et al., 2006); thus, it is unclear whether the KMN proteins regulate monopolar sister kinetochores through Sgo1.

S. pombe is an excellent system for studying meiosis because, in this organism, meiosis is easily induced and takes only 6–8 h to complete, and the entire process can be followed under a microscope. Normal yeast meiosis yields four spores (yeast gametes) in an ascus. Errors during meiotic progression result in an ascus with an abnormal number of spores, as is seen in *rec8* and *moa1* deletion mutants and recombination mutants (Watanabe and Nurse, 1999; Molnar et al., 2001b; Davis and Smith, 2003; Yokobayashi and Watanabe, 2005). In our attempt to identify spore formation mutants by deleting genes encoding nonessential nucleoporins, we identified *nup132*$^+$: loss of Nup132 results in an aberrant number of spores after meiosis (Asakawa et al., 2014). Nup132, the *S. pombe* homologue of mammalian Nup133, is a component of the Nup107-Nup160 subcomplex that constitutes the core structure of the nuclear pore complex (Baï et al., 2004; Asakawa et al., 2014). In this study, we used a live-cell imaging system to monitor the meiotic progression of a *nup132*Δ mutant and found that Nup132 modulates monopolar spindle attachment of sister kinetochores at metaphase I by regulating outer kinetochore assembly in the preceding meiotic prophase.

Results

Depletion of *nup132*$^+$ leads to SAC-dependent extension of metaphase I

To determine what causes the aberrant numbers of spores observed in the *nup132*Δ mutant, we first monitored meiotic progression in *nup132*Δ cells coexpressing fluorescently tagged tubulin and histones. Tubulin forms spindles during nuclear division, and therefore the duration from spindle formation to depolymerization was determined. As shown in Fig. 1 A, in the wild-type cell, the durations of meiosis I and meiosis II were 36 min each (0–36 min and 54–78 min, respectively). In contrast, *nup132*Δ cells frequently spent more time at each meiotic division (Fig. 1 B; 0–54 min at meiosis I and 72–126 min at meiosis II). This prolonged nuclear division is meiosis specific because the duration of mitotic division in the *nup132*Δ mutant (29 ± 3 min) was similar to that of the wild type (31 ± 3 min). By plotting spindle length over time, we identified the three phases of nuclear divisions as previously stated (Nabeshima et al., 1998; Zimmerman et al., 2004): First, spindles attach to the kinetochores and grow stably during prometaphase. Then, they are maintained at a constant length during metaphase, and, finally, they elongate at anaphase (Fig. 1 C). It appeared that in most *nup132*Δ cells, prometaphase was not affected but the duration of the constant spindle length phase (i.e., metaphase) was longer than that in the wild-type cells (Fig. 1, B and C). In the *nup132*Δ mutant, chromosomes, as observed by histone H3-mRFP, could often segregate during the prolonged meiosis I; however, chromosome segregation at meiosis II sometimes failed (~25% of the cells; Fig. 1 B, arrows). This explains a possible cause for the previously reported nontetrad formation, which also occurs at ~25% in this mutant; however, such nontetrad spores are viable (Asakawa et al., 2014; see Fig. 9).

The extended meiotic metaphase observed in the *nup132*Δ mutant infers activation of the SAC. Cells with a single deletion of one of the genes encoding the SAC components Mad2 or Bub1 underwent meiosis I at a similar time interval as wild-type cells (Fig. 1 D). In contrast, deletion of *mad2*$^+$ or *bub1*$^+$ in the *nup132*Δ background significantly shortened the prolonged meiosis I observed in the *nup132*Δ single mutant. However, prolonged meiosis II was not dependent on the SAC (Fig. 1 D). We reasoned that in the *nup132*Δ mutant, activated SAC inhibits the activity of the APC and delays the transition from metaphase I to anaphase I. To verify this, activity of the APC was monitored by using GFP-labeled Cut2/securin because it is known to localize to spindles and is abruptly degraded by the APC at the metaphase-anaphase transition in *S. pombe* (Funabiki et al., 1996). Disappearance of Cut2/se-

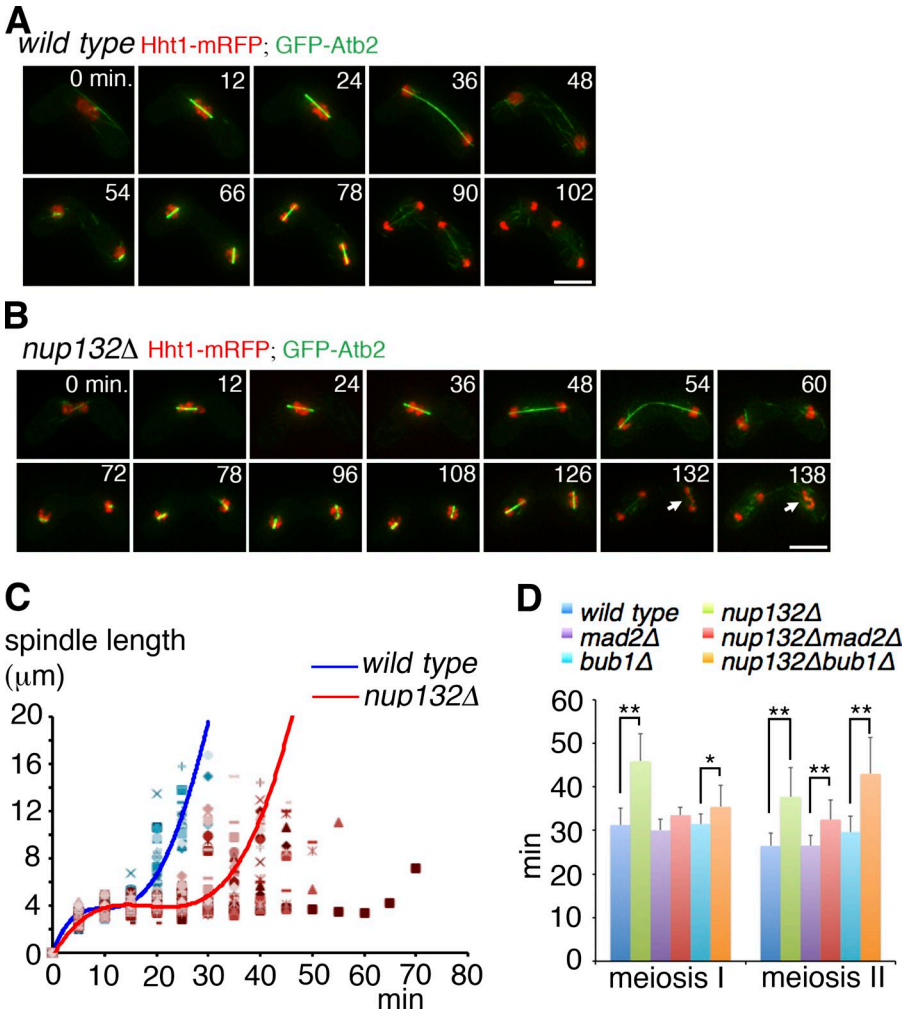

Figure 1. **Depletion of *nup132*⁺ causes SAC-dependent extension of meiosis I.** (A) Meiotic progression of a wild-type cell expressing Hht1-mRFP and GFP-Atb2. Hht1-mRFP and GFP-Atb2 were used to visualize histone H3 (shown in red) and tubulin (shown in green), respectively. The numbers shown in white are the time in minutes after the spindle first appeared (at t = 0). The duration of meiosis I and meiosis II was determined as the time from spindle formation to depolymerization. The cell in this representative image spent 36 min in meiosis I (from 0 to 36 min), and metaphase I was from 12 to 24 min. This cell spent 24 min in meiosis II (from 54 to 78 min). Bar, 5 μm. (B) A typical example of a *nup132*Δ cell undergoing prolonged meiosis I and II. The color coding for the staining is the same as in A. The duration of meiosis I for the cell in this image is 54 min (from 0 to 54 min), and metaphase I was from 12 to 36 min. The duration of meiosis II was 54 min (from 72 to 126 min). The white arrows at time points 132 min and 138 min indicate the chromosomes that failed to separate at meiosis II. Bar, 5 μm. (C) The spindle length of each cell during meiosis I was measured using DeltaVision software and plotted over time. The different symbols represent different cells. The blue symbols are wild-type cells (n = 28), and the red symbols are *nup132*Δ cells (n = 37). Third-order polynomial trend lines were used to fit the data sets. The blue line is the trend line for the wild-type cells (R^2 = 0.998), and the red line is the trend line for the *nup132*Δ cells (R^2 = 0.988). (D) Quantification of the duration of meiosis. The strains expressing mCherry-Atb2 were induced to enter meiosis, and meiotic durations were measured via time-lapsed live-cell imaging. The durations of meiosis I and II were determined as the time the spindle was present. The error bars indicate the standard deviation of at least 20 independent cells of each strain. Statistical significance was evaluated by determining the P value using Student's t test. *, P = 0.01; **, P < 0.001.

curin from the metaphase I spindles was significantly delayed when *nup132*⁺ was depleted (Fig. S1). This result suggests that the activated SAC causes the metaphase I extension observed in the *nup132*Δ mutant.

S. pombe undergoes closed nuclear divisions with the intact nuclear envelope. As *nup132*⁺ encodes a scaffold protein of the nuclear pore complex, it is possible that depletion of *nup132*⁺ disrupts the nucleocytoplasmic barrier and broadly affects the factors that regulate meiotic progression. To test this, 3GFP-NLS was used as a nuclear marker to monitor the nucleocytoplasmic barrier. In a wild-type cell, 3GFP-NLS remains in the nucleus throughout meiosis (Fig. S2 A), except for transient dispersion to the cytoplasm in anaphase II (referred to as virtual nuclear envelope breakdown in Asakawa et al., 2010). In the *nup132*Δ mutant, the nucleocytoplasmic barrier was intact during the prolonged period of metaphase I although leakage of the 3GFP-NLS signals was observed at the onset of anaphase I and during interkinesis (Fig. S2, B and C). Therefore, based on the results of the nuclear reporter assay, there is no evidence that unregulated nucleocytoplasmic transport leads to prolongation of metaphase I in the *nup132*Δ mutant.

Abnormal movement of meiosis I sister centromeres along the spindles in the *nup132*Δ mutant

SAC is activated when the tension at sister kinetochores is absent. To analyze tension at the sister kinetochores, mCherry-Atb2 and *cen2*-lacO/lacI-GFP (called *cen2*-GFP hereafter) were introduced into a heterothallic strain of a *nup132*Δ mutant. The resultant strain was then mated with GFP-negative heterothallic partners lacking *cen2*-GFP. A pair of chromosome II sister chromatids was labeled with *cen2*-GFP and distinguished from the unlabeled homologous chromosomes. The sister *cen2*-GFP quickly moved back and forth on the spindles at prometaphase I in both the wild-type and *nup132*Δ mutant cells (Fig. 2, A and B, arrowheads). However, the sister *cen2*-GFP of most wild-type cells quickly settled at one end of the spindles as meiosis I proceeded (Fig. 2, A and C), suggesting that after tension resulting from chiasmata and monopolar spindle attachment was satisfied at the sister kinetochores, the sister centromeres soon moved together to the same spindle pole. On the contrary, the sister *cen2*-GFP of the *nup132*Δ cells often wobbled along the spindle axis during the prolonged meiosis I (Fig. 2, B [arrows] and C), possibly reflecting unsatisfied

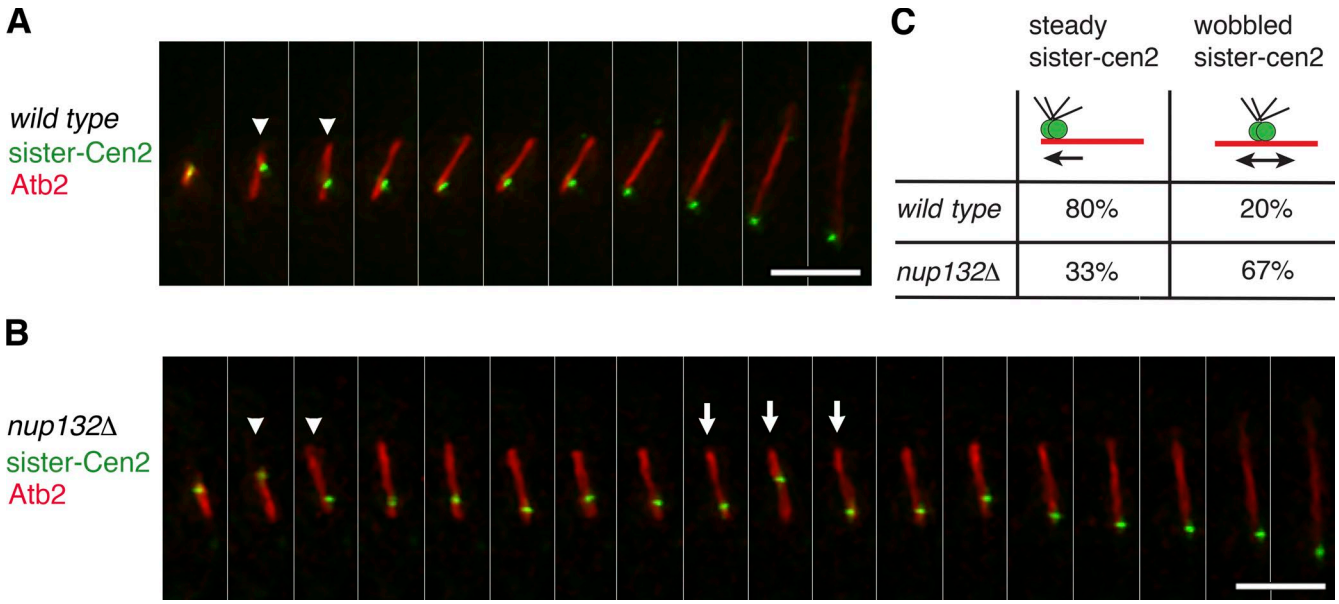

Figure 2. **Abnormal movement of sister *cen2*-GFP during meiosis I is delayed in the *nup132*Δ mutant.** (A and B) Live-cell imaging of the sister centromeres (*cen2*) of (A) wild-type or (B) *nup132*Δ heterothallic zygotes during meiosis I. The *cen2-lacO*/lacI-GFP (*cen2*-GFP) system was used to visualize the sister centromeres of chromosome II. Spindles were visualized using mCherry-Atb2. The arrowheads indicate the time points at which the sister cen2-GFP moved between the two ends of the spindles at prometaphase I. The arrows indicate the time points at which the sister cen2-GFP evidently wobbled along the metaphase spindles. Images were obtained every 2 min. Bar, 5 µm. (C) Quantification of sister *cen2*-GFP movement at metaphase I. Movement of the sister *cen2*-GFP along the meiotic spindles was categorized into two types: steady sister-*cen2* and wobbled sister-*cen2*. Steady sister-*cen2* refers to the cells whose sister *cen2*-GFP steadily settled at one end of the spindles throughout metaphase I. Wobbled sister-*cen2* are the cells with sister *cen2*-GFP moving between the two ends of the spindles during metaphase I. *n* = 20 for each strain.

tension at the sister kinetochores. These results also suggest that the sister centromeres of the *nup132*Δ mutant experienced pulling forces from the opposite spindle poles.

Normal chiasma formation in the *nup132*Δ mutant

The absence of chiasmata could result in loss of tension at sister kinetochores and activate SAC (Yamamoto et al., 2008). This prompted us to examine whether homologous chromosome recombination occurs in the *nup132*Δ mutant; this was done using Rhp51-ECFP as a DSB repair marker (Akamatsu et al., 2007). Both the *nup132*Δ mutant and wild-type cells accumulated bright punctate signals of Rhp51-ECFP in the nuclei during meiotic prophase, indicative of repairing of DSB (Fig. 3, A and B). As a negative control, Rhp51-ECFP appeared to be uniformly distributed in the nucleus of the *rec12*Δ mutant, which does not initiate meiotic DSBs (Fig. 3 C). The punctate signals were greatly reduced by the time of telomere dispersal (i.e., at the end of meiotic prophase) and totally disappeared at anaphase I (Fig. 3, A and B), suggesting that the DSBs were repaired by homologous chromosome recombination. In agreement with this, recombinant gametes were frequently observed in the *nup132*Δ mutant, although the recombination rate was slightly decreased compared with that in the *wild-type* strain (Fig. 3 D). These results demonstrate that activation of SAC in the *nup132*Δ mutant is not due to a lack of chiasmata.

The sister centromeres maintain cohesion in the *nup132*Δ mutant

We then investigated whether the wobbled movement of the sister *cen2*-GFP in meiosis I resulted from a premature loss of the meiotic cohesin Rec8. Localization of Rec8-GFP in the mutant was examined. In both wild-type and *nup132*Δ cells, Rec8-GFP localized along the chromosomes during meiotic prophase and metaphase and then suddenly disappeared from the chromosome arms, but it remained at the centromeres at anaphase I (Fig. 4, A and B). The centromeric localization of the Rec8 protector Sgo1 and the Rec8-interacting protein Moa1 was also not affected in the *nup132*Δ mutants (Fig. S3). To further confirm this result, we performed a cohesin assay in cells with the *mes1*Δ homothallic strain background expressing *cen2*-GFP. *mes1*$^+$ was deleted to arrest the cells before the onset of meiosis II (Kitajima et al., 2004). The *bub1*Δ*mes1*Δ mutant was used as a positive control for the assay because the centromere localization of Rec8 precociously disappears in meiosis I in the absence of Bub1 (Kitajima et al., 2004). Two separate dots were frequently observed in the divided meiosis I nuclei of the *bub1*Δ*mes1*Δ mutant, indicating precocious splitting of the sister *cen2* caused by the loss of Rec8 in meiosis I. The sister *cen2*-GFP remained close and appeared as a single dot or as a pair of neighboring dots in the divided meiotic nuclei of the *mes1*Δ or *nup132*Δ*mes1*Δ cells (Fig. 4, C and D). These results indicate that, in the absence of *nup132*$^+$, Rec8 remains intact in the centromere region in meiosis I.

Precocious appearance of outer kinetochore proteins during meiotic prophase in the *nup132*Δ mutant

Reorganization of the meiotic kinetochores has been implicated in the regulation of monopolar spindle attachment. The KMN proteins in the outer kinetochores are disassembled at early meiotic prophase and are reassembled before the onset of metaphase I (Hayashi et al., 2006). Therefore, we examined the meiotic behaviors of the KMN components Mis12 and Spc7 in the *nup132*Δ mutant. GFP-tagged Mis12 or Spc7 was introduced into cells carrying Cut11-mCherry. Cut11 is a nucleop-

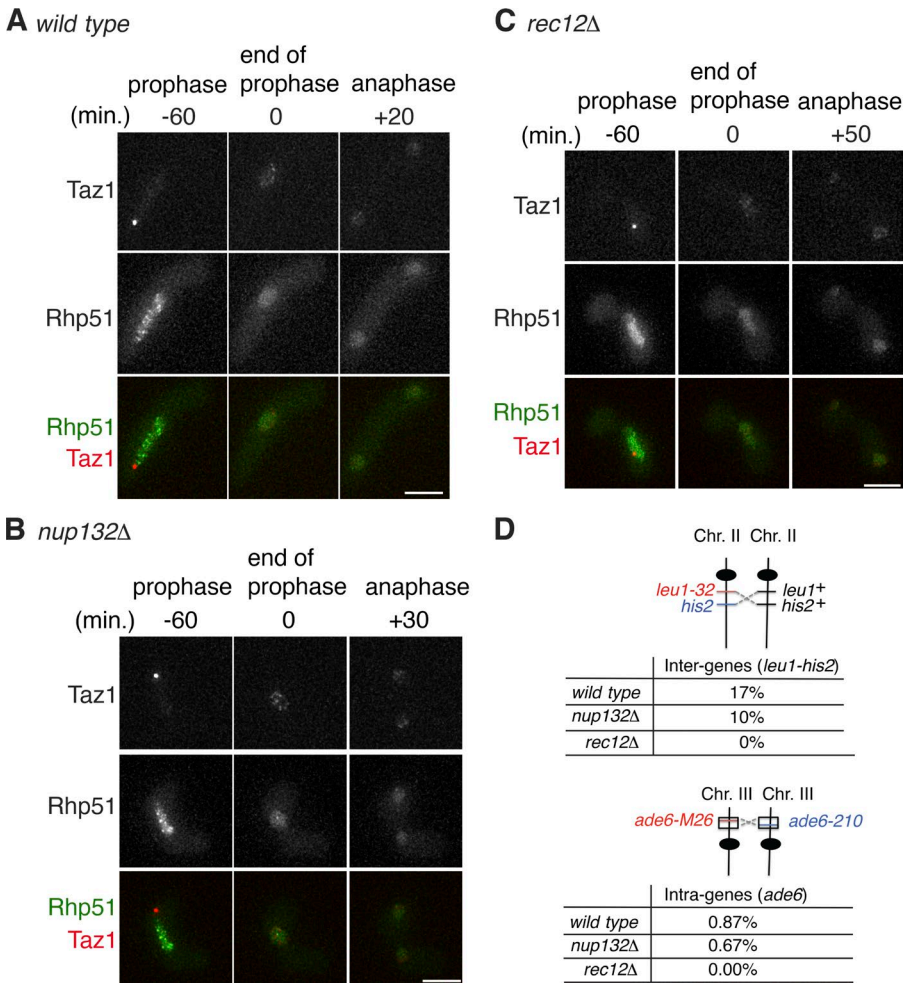

Figure 3. **The *nup132*Δ mutant is not achiasmate.** (A–C) Meiotic DSB formation was examined by imaging foci formation of Rhp51-ECFP in wild-type (A), *nup132*Δ (B), and *rec12*Δ (C) cells. Meiotic prophase is characterized by a bright Taz1-mCherry signal at telomeres, and dispersal of the Taz1 signals (telomere declustering) designates the end of prophase (t = 0). Bar, 5 µm. (D) Tetrad analysis was performed to determine the genetic distance between *leu1* and *his2* (intergenic recombination rate), whereas the allelic intragenic recombination rate of *ade6* was determined by a random spore assay. The chromosomal positions in genes related to centromeres (black circles) are shown. "Wild-type" refers to the crosses between CRL134 (*his2 leu1-32 ade6-M26*) and AY116-11A (*ade6-210*), whereas "*nup132*Δ" refers to the crosses between HJY389 (*his2 leu1-32 ade6-M26 nup132*Δ) and HJY388 (*ade6-210 nup132*Δ). The "*rec12*Δ" strain, which is a cross between HJY612 and HJY617, serves as a negative control for the recombination assay. The recombination rate of *leu1-his2* is the percentage of recombinant tetrads observed (number of tetrads observed >50 for each cross). To determine the *ade6* allelic intragenic recombination rate, random spores were first plated on YES plates to allow colony formation. The colonies on the YES plates were replica plated onto yeast extract (YE). The *ade6* intragenic recombination rate is the percentage of white colonies formed on the YE plates (n > 1,200 colonies).

orin protein that localizes to the nuclear envelope throughout the cell cycle and to the SPB during metaphase (West et al., 1998). Thus, it was used to define the nuclear region and determine the timing of meiotic progression (i.e., karyogamy, meiotic prophase, and prometaphase). As previously reported (Hayashi et al., 2006), in wild-type cells, the Mis12-GFP and Spc7-GFP signals disappeared from the centromeres upon karyogamy and did not reappear until meiosis I onset (Fig. 5, A and B). Remarkably, 53% of *nup132*Δ cells had Mis12-GFP signals (Fig. 5, C and E), and 77% of *nup132*Δ cells had Spc7-GFP signals in the nuclei at early meiotic prophase (Fig. 5, D and F). The times of the first appearances of Mis12-GFP and Spc7-GFP signals are plotted in Fig. 5, E and F. These GFP foci of Mis12 or Spc7 localized to one of the centromeres, which were visualized by the mCherry-tagged constitutive inner-kinetochore protein Mis6, but not to all of the centromeres (Fig. 6). These results suggest that Mis12 and Spc7 precociously assembled to, or never disassembled from, some of the centromeres in the absence of Nup132.

The phenotype of precocious meiotic kinetochore assembly is unique to the *nup132*Δ mutant. Deletion of any of the five genes encoding other nonessential nucleoporins, *ely5*$^+$, *nup37*$^+$, *pom152*$^+$, *nup124*$^+$, and *nup61*$^+$, which when deleted give rise to abnormal spore numbers (Asakawa et al., 2014), did not affect Mis12-GFP dissociation/association at the centromeres. Moreover, neither *rec8*Δ nor *rec12*Δ displays the phenotype of precocious Mis12 reappearance at the centromeres (Fig. S4). Therefore, Nup132 regulates meiotic outer kinetochore reorganization independent of the Rec8-mediated pathway or chiasmata formation.

The partially preassembled outer kinetochores of the *nup132*Δ mutant are separated from the SPB

Another KMN component, Nuf2, which connects the centromeres to the SPB, disappears at the early meiotic prophase and releases the centromeres from the SPB (Asakawa et al., 2005; Hayashi et al., 2006). In wild-type cells, similar to Mis12-GFP and Spc7-GFP, the Nuf2-GFP signals disappeared at early meiotic prophase and reappeared at the later stage of meiotic prophase I (~40 min before metaphase I onset; Fig. 7 A). In the *nup132*Δ mutant, the meiotic behavior of Nuf2-GFP was normal, similar to that observed in the wild-type strain (Fig. 7, B and C). Ndc80, the Nuf2 interacting protein, also behaved normally in the mutant (Fig. 7 C). In addition, the Csi1 protein, which is a kinetochore-SPB connector in mitotic interphase (Hou et al., 2012), disappeared at early meiotic prophase (Fig. S5). Csi1-mCherry signals reappeared in late meiotic prophase before telomere dispersal and colocalized with the telomere marker Taz1-GFP (Fig. S5). Because telomeres are clustered at the SPB during meiotic prophase (Chikashige et al., 1997), colocalization of Csi1-mCherry and Taz1-GFP suggests that Csi1 reassembled to the SPB during meiotic prophase. The meiotic behavior of Csi1 in the *nup132*Δ mutant was the same as that

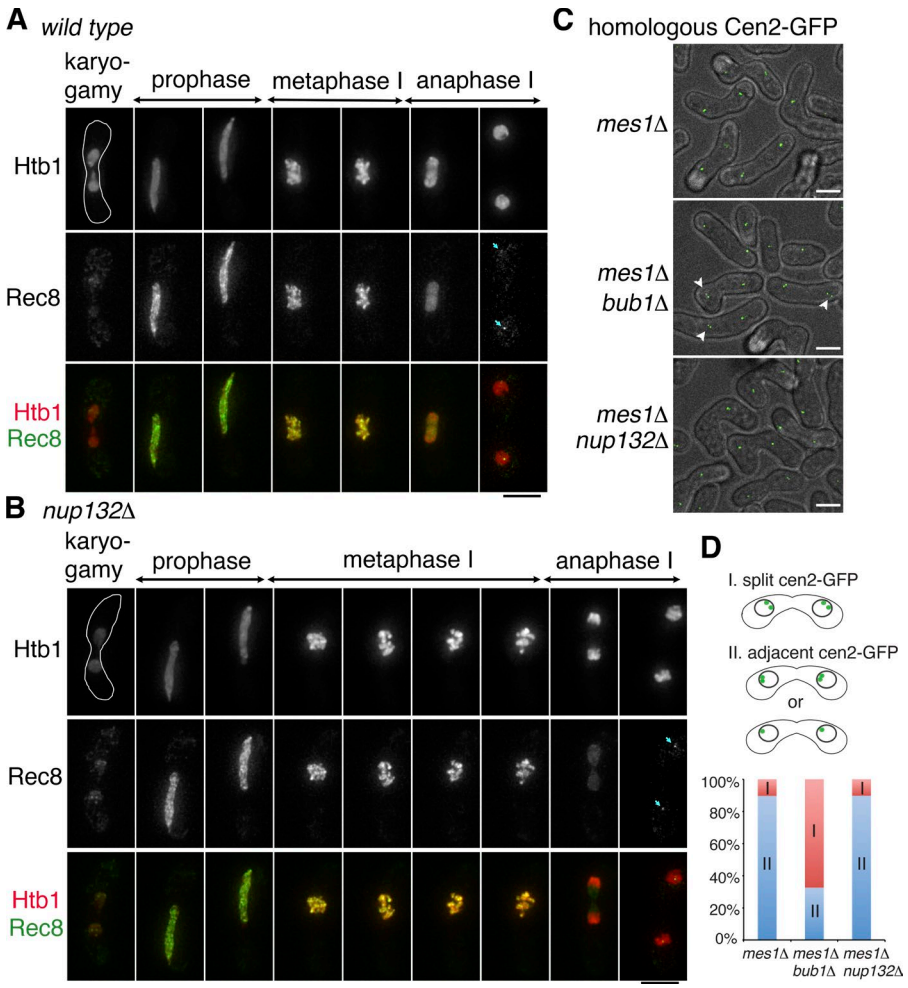

Figure 4. **Centromere cohesin remained intact at the completion of meiosis I in the *nup132*Δ mutant.** (A) An example of a wild-type cell undergoing meiosis I. Htb1-mCherry and Rec8-GFP were used to visualize histone H2B (red) and meiotic-specific cohesin (green), respectively. Meiotic stages are defined by the behavior of chromosomes. Karyogamy is the stage when the two haploid nuclei fuse. Prophase is the stage when the elongated horsetail-shaped nucleus moves back and forth. Metaphase I is defined by chromosome condensation, and anaphase I is the stage when the nucleus stretches and divides into two nuclei. The cyan arrows in anaphase I indicates the remaining GFP signals of centromeric Rec8. Bar, 5 µm. (B) Representative time-lapse images of a *nup132*Δ cell expressing Htb1-mCherry and Rec8-GFP during meiosis I. All the labels are described as in A. Bar, 5 µm. (C) Representative views of cells carrying homologous *cen2-lacO*/lacI-GFP (*cen2*-GFP) at meiosis I. The *cen2*-GFP signals can be seen as white dots inside the cells. Bright-field images were combined with the GFP fluorescence images so that the cell outline can be viewed. The *mes1*Δ background was used to stop the cells from entering meiosis II after completion of meiosis I. After meiosis I, the homologous *cen2*-GFP signals split into two, whereas the sister *cen2*-GFP remains together or closely adjacent. The *bub1*Δ strain was used as a negative control. The white arrowheads indicate separating sister *cen2*-GFP in *mes1*Δ *bub1*Δ cells. Bars, 5 µm. (D) The upper diagram illustrates two types of cells carrying homologous *cen2*-GFP after meiosis I. The type I cells are those with more than two separated dots of *cen2*-GFP in each of the divided nuclei (i.e., a split *cen2*-GFP). The type II cells are those with one dot or two closely adjacent dots in each of the divided nuclei (i.e., adjacent *cen2*-GFP). The lower diagram shows the percentage of type I and type II cells in the *mes1*Δ, *mes1*Δ*bub1*Δ, or *mes1*Δ*nup132*Δ mutant background ($n = 75$ for each strain).

observed in the wild-type strain (Fig. 7 F). Thus, in the mutant, both Nuf2 and Csi1 are properly disassembled early in meiotic prophase and do not reassemble until late in meiotic prophase. Consistent with the fact that Nuf2 and Csi1 are required for the centromere-SPB connection, the centromeric foci of Mis12-GFP or Spc7-GFP did not colocalize with the SPB component Sfi1 or the telomere-bound protein Taz1 (Fig. 7, D and E), indicating that centromeres partially preassembled with Mis12 and Spc7 are not connected to the SPB in early meiotic prophase when Nuf2 and Csi1 are not reassembled at the centromeres.

Early recruitment of Bub1 in the *nup132*Δ mutant

Spc7 directly interacts with the SAC component Bub1 (Shepperd et al., 2012). Because Spc7 is precociously loaded onto the centromeres in the *nup132*Δ mutant, we wondered if Bub1 is also precociously recruited. Similar to the KMN proteins, Bub1-GFP signals appeared as foci in the nucleus shortly before the onset of metaphase I in the wild-type cells (Fig. 8 A), suggesting that Bub1 is recruited to the kinetochores when the KMN proteins reassemble. In the *nup132*Δ mutant, the Bub1-GFP signals appeared at early meiotic prophase (Fig. 8, B and C), indicating that Bub1 is precociously recruited to the centromeres. Nevertheless, Sgo1-GFP signals appeared at the normal time in the *nup132*Δ mutant (Fig. 8 D). These results suggest that the early recruitment of Bub1 in the *nup132*Δ mutant is not sufficient to recruit Sgo1 to the preassembled kinetochores and that the defective meiotic kinetochore in *nup132*Δ forms without affecting Sgo1.

Equational chromosome segregation in meiosis I is drastically increased when *nup132*$^+$ is depleted in the *bub1*Δ background

We reasoned that precocious assembly of kinetochores might affect subsequent monopolar microtubule-kinetochore attachment. To determine whether the deletion of *nup132*$^+$ affected sister chromatid segregation in meiosis I, the segregation pattern of the sister *cen2*-GFP in meiosis I was determined using live-cell imaging. Coexpression of Cut11-mCherry was used to outline the meiosis I nuclei. Normally, when monopolar spindle attachment of sister chromatids is established in meiosis I, the sister *cen2*-GFP cosegregates to the same nucleus (Fig. 9 A, top and wild type). In contrast, if bipolar spindle attachment of sister chromatids is established, precocious sister chromatid segregation (i.e., equational segregation) may occur. As shown

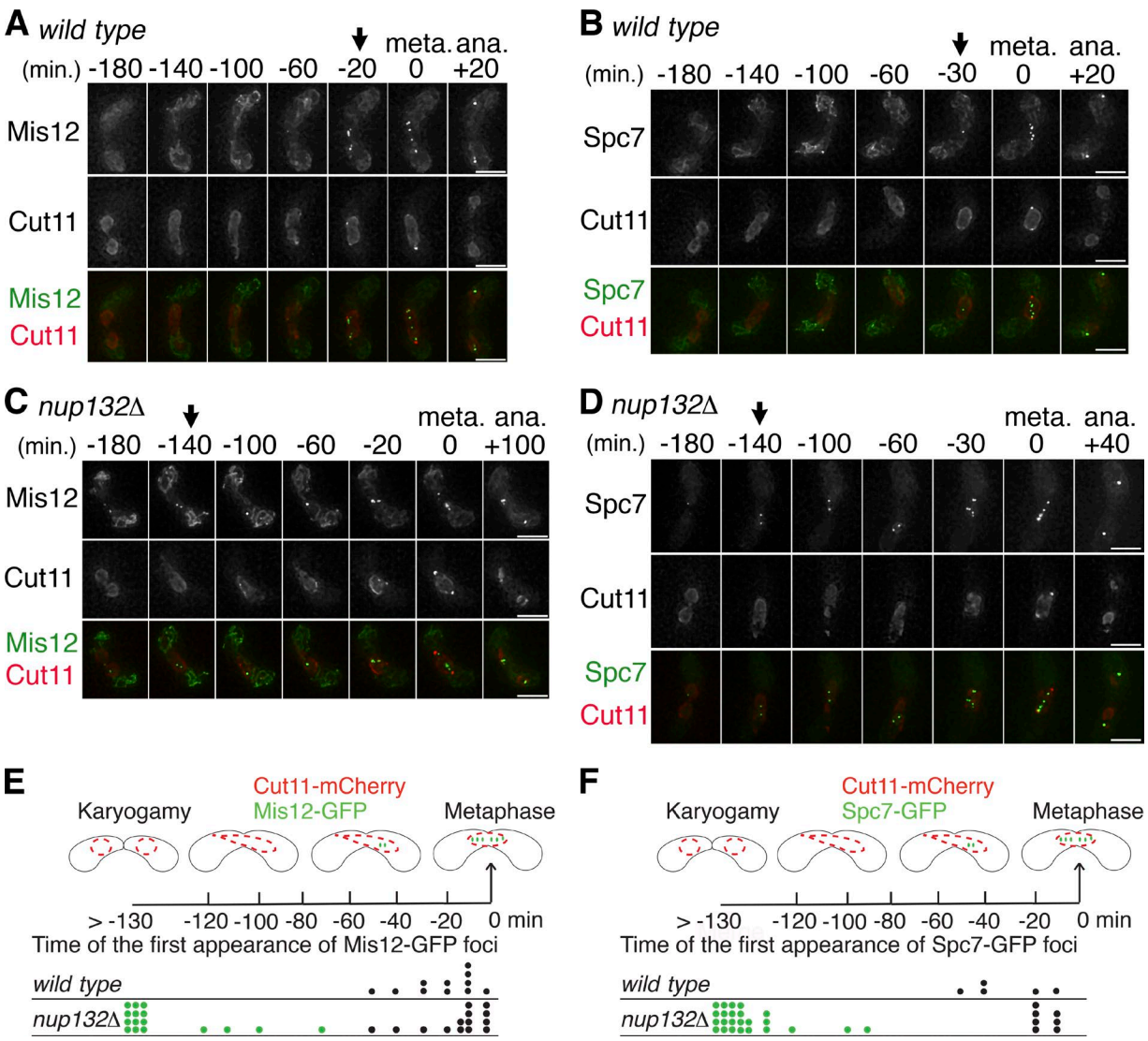

Figure 5. **Precocious assembly of Mis12 and Spc7 at the meiotic centromeres in the *nup132*Δ mutant.** (A and B) Live-cell imaging of wild-type cells expressing mCherry-tagged Cut11 and GFP-tagged Mis12 (A) or Spc7 (B). The numbers at the top indicate the time in minutes. Time 0 is the beginning of metaphase (meta). The nucleus is outlined by the Cut11-mCherry signals. The black arrow signifies the time when the GFP signals were first observed at the centromeres. The green and red colors in the merged images represent the GFP-tagged and mCherry-tagged proteins, respectively. Bars, 5 µm. (C and D) Representative meiotic behaviors of GFP-tagged Mis12 (C) or Spc7 (D) in the *nup132*Δ mutant. All the label descriptions are as in A. Bars, 5 µm. (E and F) Time points at which the Mis12-GFP (E) and Spc7-GFP (F) foci first appeared. The nuclear dynamics of meiotic cells is illustrated along a time line where time is shown in minutes before the beginning of metaphase. In the upper panel, the red-dashed line represents the nucleus, as outlined by the Cut11-mCherry signals, and the green dots represent the GFP foci. In the lower panel, the time points at which the Mis12-GFP foci (E) and Spc7-GFP foci (F) first appeared are plotted along the time line until the beginning of metaphase. Each spot represents a time point in one of the observed zygotes. The black spots represent the cells in which the GFP foci first appeared within 60 min before the beginning of metaphase (t = 0), which were considered normal. The green spots represent the cells in which the GFP foci first appeared earlier than 60 min before the beginning of metaphase. ana, anaphase.

in Fig. 9 A, the sister *cen2*-GFP of a *nup132*Δ or a *mad2*Δ single mutant cosegregated to the same nucleus with high fidelity. Nevertheless, the frequency of equational segregation in meiosis I increased to 7% in the *nup132*Δ*mad2*Δ double mutant. This result suggests that erroneous microtubule-kinetochore attachments occurred in the *nup132*Δ mutant but that the erroneous attachments can be corrected in the presence of SAC.

In addition to SAC, sister centromere coherence prevents equational segregation of the sister chromatids in meiosis I. We therefore examined the segregation pattern of sister *cen2*-GFP in the *sgo1*Δ background, in which sister centromere cohesion is compromised (Kitajima et al., 2004). As previously reported (Kitajima et al., 2004), *sgo1*$^+$ deletion alone subtly disturbed the segregation pattern of the sister *cen2*-GFP. Noticeably, for the deletion of *mad2*$^+$ in the *sgo1*Δ background, the frequency of equational separation increased to 15% (Fig. 9 A), confirming that both SAC and sister centromere coherence contribute to the cosegregation of sister chromatids in meiosis I. Consistent with this, the depletion of Bub1, which functions upstream of Mad2 and Sgo1, also led to increased frequency of equational segregation, similar to that of the *mad2*Δ*sgo1*Δ double mutant (Fig. 9 A).

Deletion of *nup132*$^+$ did not exacerbate the level of equational segregation of the sister *cen2*-GFP in the *sgo1*Δ or *mad2*Δ*sgo1*Δ background. However, the deletion of *nup132*$^+$ in the *bub1*Δ background drastically increased the frequency

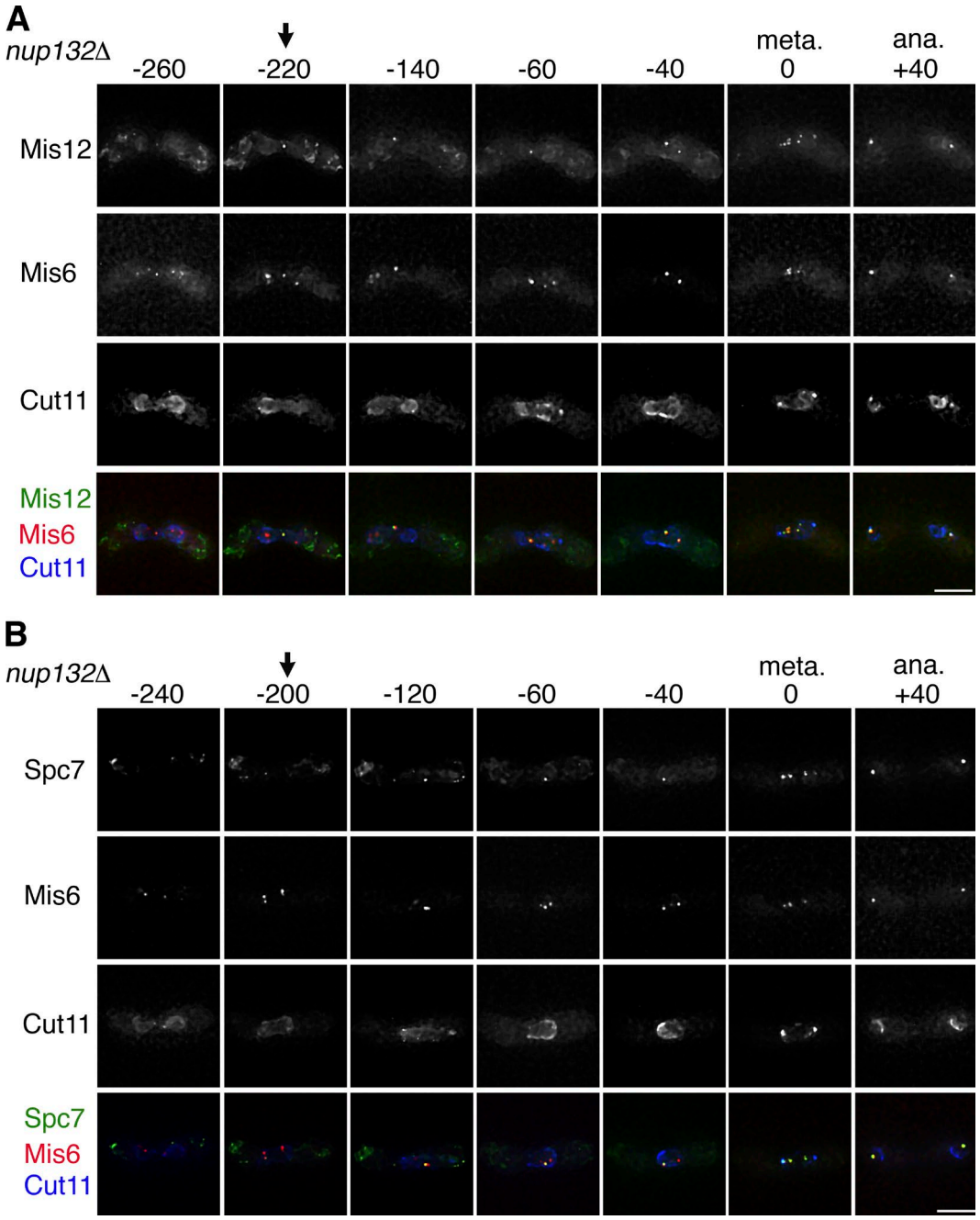

Figure 6. **Mis12 and Spc7 precociously localize to the centromeres at early meiotic prophase in the *nup132*Δ mutant.** (A and B) Mis12-GFP (A) or Spc7-GFP (B) colocalized with Mis6-mCherry in the *nup132*Δ mutant. The numbers at the top indicate the time in minutes. Time 0 is the beginning of metaphase. CFP-tagged Cut11 (blue) outlines the nucleus. The arrows indicate the first time points at which Mis12-GFP was observed as a focus in the nucleus. Bars, 5 µm. ana, anaphase; meta, metaphase.

of equational segregation in meiosis I, and the sister chromatids were randomly segregated (i.e., ∼50% cosegregation and 50% equational segregation; Fig. 9). In addition to functioning in SAC and Sgo1 recruitment, *bub1*$^+$ appears to act synergistically with *nup132*$^+$ to modulate meiotic microtubule-kinetochore attachment (see Discussion).

Discussion

In this study, we performed live-cell imaging analysis of meiosis in the *S. pombe nup132*Δ mutant and showed that depletion of Nup132 increased the duration of the meiotic divisions. Meiosis I is prolonged as a result of SAC activation, whereas meiosis II prolongation is not SAC dependent. At least two possible reasons could account for the prolonged meiosis II observed in the *nup132*Δ mutant: first, the second meiotic divisions are impeded by errors that result from meiosis I chromosome segregation; and second, the untimely breakage of the nucleocytoplasmic barrier during interkinesis interferes with the normal progression of meiosis II (Fig. S2). Currently, we cannot determine whether either of these is the major cause of meiosis II nuclear division failure that leads to nontetrad formation in the *nup132*Δ mutant.

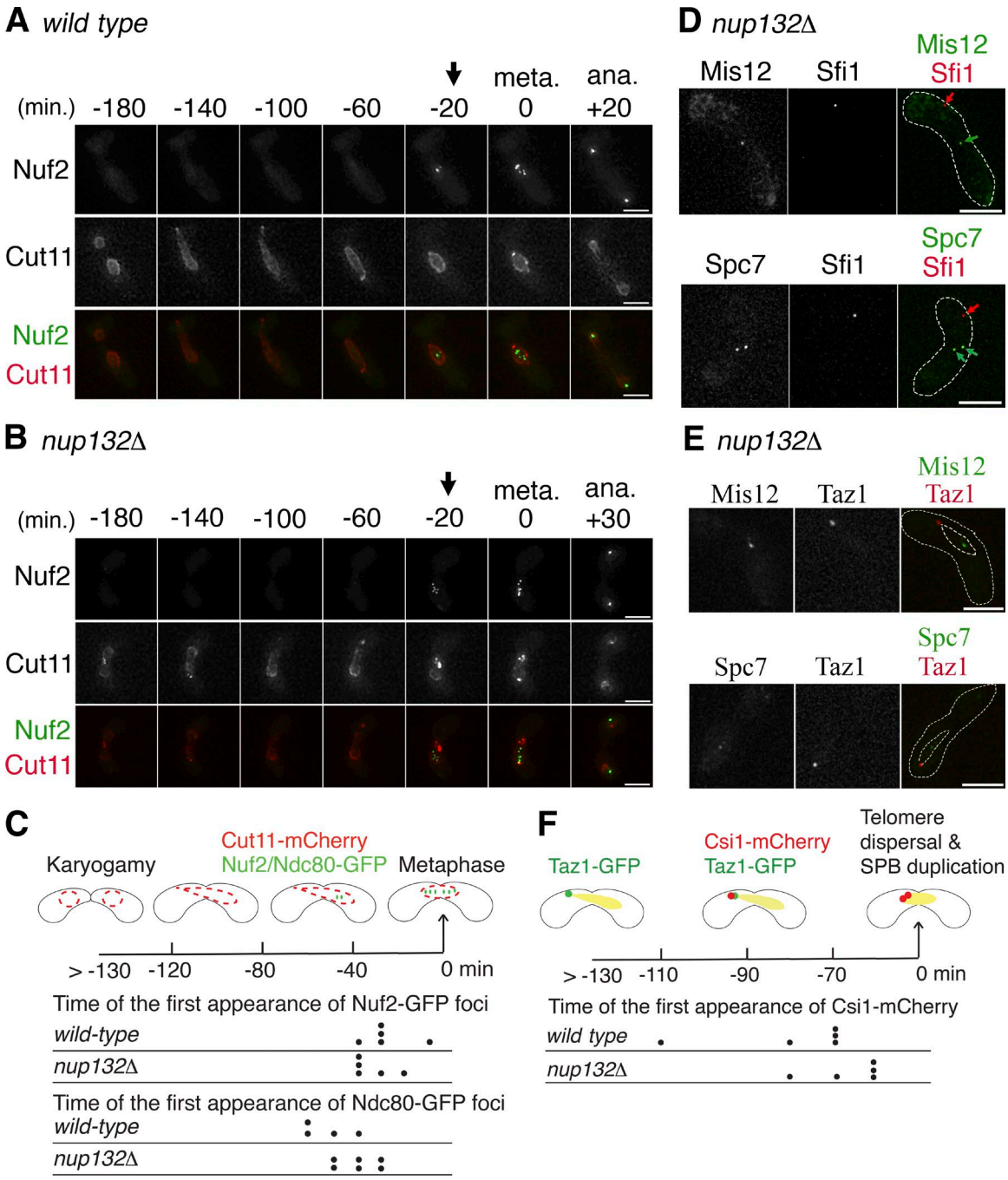

Figure 7. **Behavior of Nuf2 in the wild-type strain and *nup132*Δ mutant.** (A and B) Live-cell imaging of mCherry-tagged Cut11 and GFP-tagged Nuf2 in meiotic cells of the wild-type strain (A) and the *nup132*Δ mutant (B). The numbers at the top indicate the time in minutes; 0 indicates the beginning of metaphase (meta). The nucleus is outlined by the Cut11-mCherry signals. The black arrow indicates the time when the GFP signals are first observed at the centromeres. Bars, 5 µm. (C) Time points at which the Nuf2-GFP or Ndc80-GFP foci first appeared. The nuclear dynamics of meiotic cells is illustrated along a time line where time is shown in minutes before the beginning of metaphase. In the upper panel, the red-dashed line represents the nucleus, as outlined by the Cut11-mCherry signals, and the green dots represent the GFP foci. In the lower panel, the time points at which the GFP foci first appeared are plotted along the time line until the beginning of metaphase. Each black spot represents a time point in one of the observed zygotes. (D) In the *nup132*Δ mutant, GFP-tagged Mis12 or Spc7 is localized away from the SPB marker (mRFP-tagged Sfi1) during meiotic prophase. The red arrows indicate the Sfi1 signals, and the green arrows indicate the Mis12 or Spc7 signals. The white-dashed line outlines the zygote. Bars, 5 µm. (E) In the *nup132*Δ mutant, GFP-tagged Mis12 or Spc7 is not colocalized with the telomere marker (mCherry-tagged Taz1) during meiotic prophase. The white-dashed line outlines the zygote and the nucleus. Bars, 5 µm. (F) Time points at which the Csi1-mCherry foci first appeared. The localization of Taz1 and Csi1 in meiotic cells is illustrated along a time line where the time is shown in minutes before the beginning of metaphase. In the upper panel, the green and red dots represent the Taz1-GFP and Csi1-mCherry signals, respectively. Taz1-GFP is a telomere marker, and Csi1-mCherry marks the SPB. Time zero is defined as the time at which the Taz1 signals disperse, which indicates the end of meiotic prophase. In the lower panel, the time points at which the Csi1-mCherry foci first appeared are plotted along the time line until the beginning of metaphase. Each black spot denotes a time point in one of the observed zygotes. ana, anaphase.

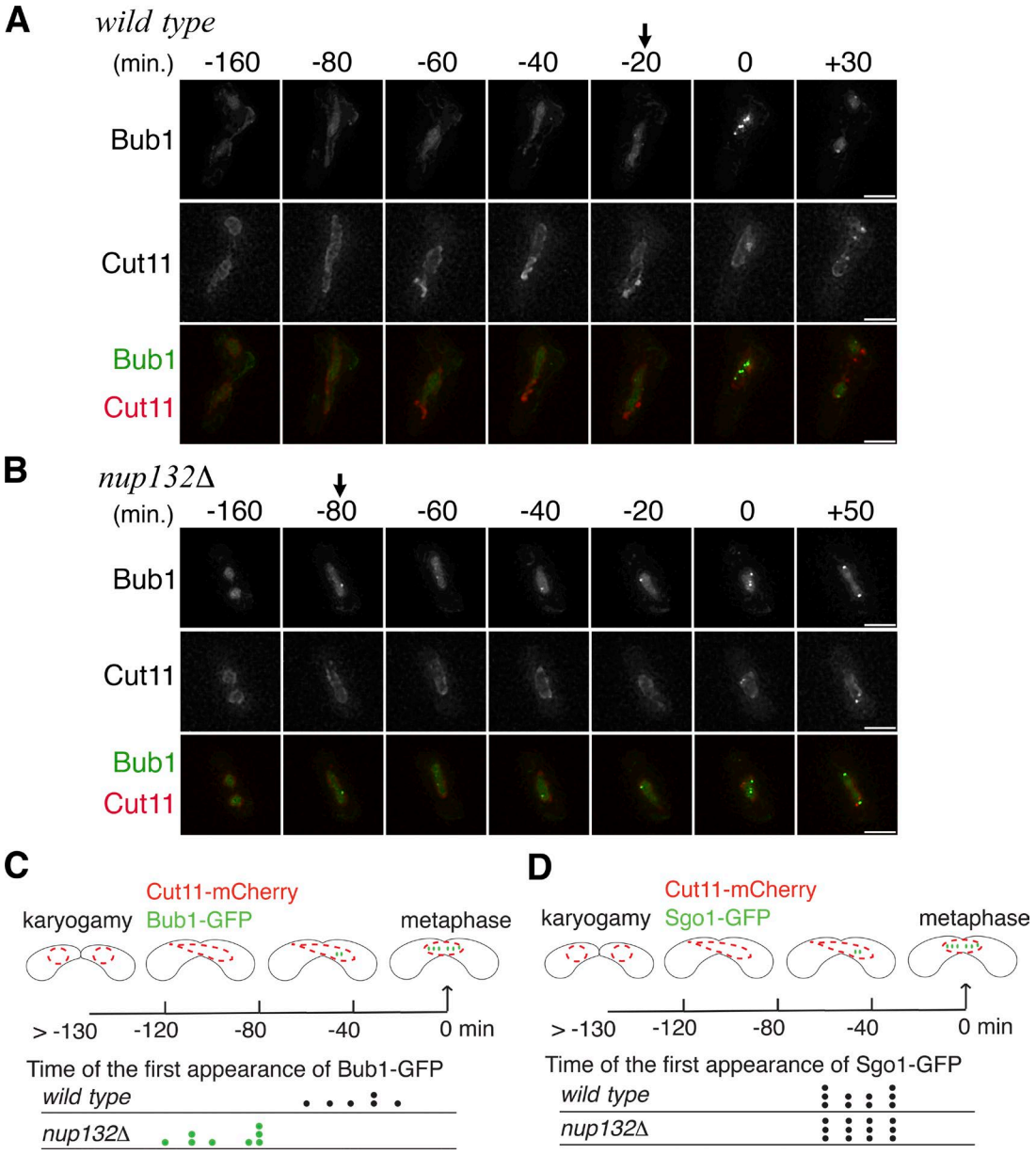

Figure 8. **Precocious localization of Bub1 at early meiotic centromeres in the *nup132*Δ mutant.** (A and B) Live-cell imaging of Bub1-GFP in meiotic cells of the wild-type strain (A) and the *nup132*Δ mutant (B). The numbers at the top indicate the time in minutes; 0 indicates the beginning of metaphase. The nucleus is outlined by the Cut11-mCherry signals. The black arrow signifies the time at which the GFP signals are first observed at the centromeres. Bars, 5 µm. (C) Time point at which the Bub1-GFP foci first appeared before the beginning of metaphase. The nuclear dynamics of meiotic cells is illustrated along a time line (time is shown in minutes). The red-dashed circles represent the nuclei, and the green dots represent the GFP foci. Each filled circle represents a zygote. The positions of the circles correspond to the time points at which the GFP foci first appeared. The black filled circles represent the cells in which the Bub1-GFP first appeared within the 60 min before metaphase began (time = 0). The green filled circles represent the cells in which the GFP foci first appeared earlier than 60 min before metaphase began. (D) Time point at which the Sgo1-GFP foci first appeared before the beginning of metaphase. The illustration is similar to that described in C.

The SAC-dependent extension of meiosis I observed in the mutant suggests increased erroneous microtubule-kinetochore attachments. In support of this notion, when SAC is absent, as in the *bub1*Δ or *mad2*Δ background, the depletion of Nup132 could lead to equational segregation of sister chromatids in meiosis I. This equational segregation was not a result of compromised sister centromere coherence because precocious splitting of *cen2*-GFP was rarely observed in the *nup132*Δ mutant.

Strikingly, in the *nup132*Δ*bub1*Δ mutant, the sister chromatids segregated almost randomly in meiosis I, which was in contrast to the relatively mild phenotype observed in the *nup132*Δ*mad2*Δ mutant. The differences were not simply caused by defects in Sgo1 recruitment to the centromeres in the *bub1*Δ mutant because, unlike the *nup132*Δ*bub1*Δ mutant, the triple mutant of *nup132*Δ*mad2*Δ*sgo1*Δ did not show random segregation of the sister chromatids. Yet, the meiosis I equational segregation in *bub1*Δ is thought to be defective in establishing an integrated sister kinetochore for sister chromatids (Bernard et al., 2001). It is possible that, in the *nup132*Δ*bub1*Δ mutant, the sister kinetochores were not properly formed, leading to random sister chromatid segregation in meiosis I. This might reflect the untimely meiotic kinetochore assembly observed in the *nup132*Δ mutant.

A

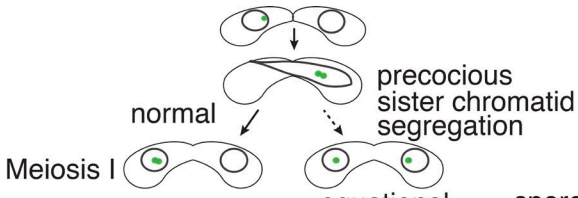

	co-segregation	equational segregation	spore viability
wild-type	100%	0%	100%
nup132Δ	100%	0%	100%
mad2Δ	100%	0%	100%
nup132Δmad2Δ	93%	7%	100%
sgo1Δ	98%	2%	48%
nup132Δsgo1Δ	96%	4%	28%
mad2Δsgo1Δ	85%	15%	61%
nup132Δmad2Δsgo1Δ	86%	14%	44%
bub1Δ	83%	17%	61%
nup132Δbub1Δ	56%	44%	51%

B

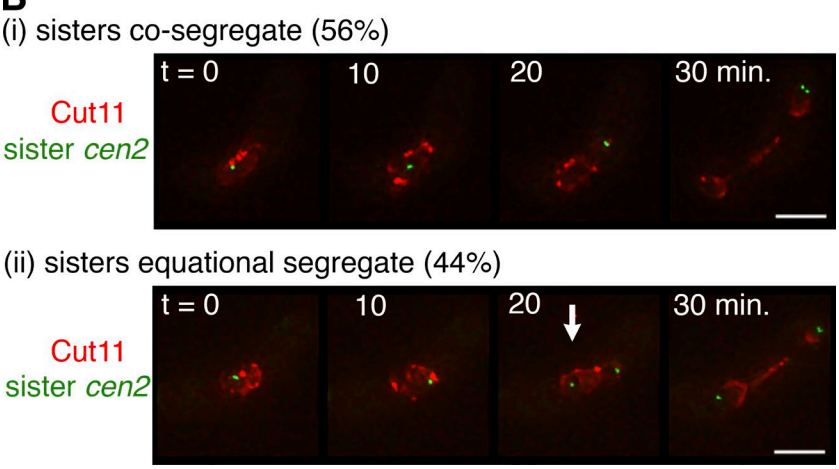

Figure 9. **Sister chromatid segregation patterns in meiosis I in various mutant backgrounds.** (A) The upper diagram illustrates a zygote formed by the mating of a heterothallic strain carrying *cen2*-GFP (green dot) with an unlabeled cell. The zygote subsequently undergoes DNA replication and enters meiosis. Owing to chromosome replication, a green dot of *cen2*-GFP becomes two green dots, one on each of the duplicated sister chromatids. Normally, the two green dots segregate to the same nucleus (black round circles) at meiosis I (i.e., cosegregation). However, if precocious sister chromatid segregation occurs, the two green dots separate into the divided nuclei at meiosis I (i.e., equational segregation). The lower diagram lists the percentages of zygotes whose sister chromatids either cosegregated or segregated equationally ($n > 40$ for each strain). The spore viability for each strain was measured by a random spore assay (See Materials and methods). (B) Representative live-cell images of sister *cen2*-GFP segregation in the *nup132Δbub1Δ* mutant. Cut11-mCherry was coimaged to outline the meiosis I nuclei. Precocious splitting of the sister *cen2*-GFP was observed in the *nup132Δbub1Δ* double mutant at the onset of anaphase I (arrow). The sister *cen2*-GFP was (i) cosegregated to the same nucleus or (ii) separated to the two divided nuclei at the completion of meiosis I. Bars, 5 µm.

Failure to disassemble the KMN complex at the kinetochores could result in precocious sister chromatid segregation (Chikashige et al., 2004; Hayashi et al., 2006). Consistently, we observed precocious assembly of the KMN proteins Mis12 and Spc7 at the meiotic centromeres in the *nup132Δ* mutant. Interestingly, our results showed that Rec8 and Rec12 are not involved in outer kinetochore reorganization during meiotic prophase and that depletion of Nup132 neither disturbs the centromere localization of Rec8 nor affects chiasmata formation. Therefore, we propose that independent of centromeric cohesin and the recombination pathway, Nup132 regulates the assembly of the KMN complex at early meiotic prophase to modulate monopolar spindle attachment in meiosis I.

Upon mating pheromone signaling, Nuf2, Mis12, and Spc7 disassemble from the centromeres and then return to the centromeres late in meiotic prophase (Hayashi et al., 2006). In the absence of Nup132, whereas Nuf2 remains dissociated from the centromeres until late meiotic prophase, Mis12 and Spc7 often appear at the centromeres early in meiotic prophase, and these partially assembled centromeres remain separated from the SPB. In this scenario, Nuf2 dissociation releases the centromeres from the SPB, and Nup132 prevents Mis12 and Spc7 from precociously assembling to the centromeres in early meiotic prophase. Bub1 is recruited early to the centromeres partially assembled with Mis12 and Spc7. Thus, Mis12 and Spc7 likely provide an interaction hub for the recruitment of SAC components. However, the timing of Sgo1 appearance was not affected by the absence of Nup132. Hence, it is likely that reorganization of the meiotic outer kinetochore modulates monopolar spindle attachment independent of Sgo1.

The metazoan homologues of Nup132 localize to the NPCs during interphase and were enriched at the kinetochores during mitosis (Belgareh et al., 2001; Mishra et al., 2010; Ródenas et al., 2012). In contrast, *S. pombe* Nup132 localizes to the NPCs throughout mitosis and meiosis, and there is no evidence of kinetochore localization (Asakawa et al., 2010, 2014). How Nup132 regulates outer kinetochore disassembly without localizing at the kinetochores is not yet known. One possible explanation is that Nup132 mediates the localization of the kinetochore proteins by sequestering them at the NPCs. Interestingly, it has been reported that the human homologue of Nup132, hNup133, interacts with the outer kinetochore protein CENP-F at the nuclear envelope (Zuccolo et al., 2007; Bolhy et al., 2011). Although there is no obvious CENP-F homologue in *S. pombe*, we noted a distant homology between human CENP-F and *S. pombe* Spo15 using a DELTA-BLAST search

(Boratyn et al., 2012). Spo15 is required for spore formation and localizes to the SPB throughout mitosis and most of meiosis (Ohta et al., 2012). Thus, Spo15 can be a candidate for a functional homologue of CENP-F that participates in outer kinetochore reorganization during meiotic prophase in *S. pombe*. However, this remains to be tested.

The *nup132*Δ mutant exhibits different effects in mitosis and meiosis (i.e., normal progression of mitosis but delays in the metaphase-anaphase transition in meiosis). This may result from differences in the dynamic nature of the outer kinetochores between mitosis and meiosis in *S. pombe*: Although the outer kinetochore dynamically disassembles and reassembles during meiotic prophase, it is a stable structure that constantly associates with the SPB during the mitotic cell cycle (Asakawa et al., 2007). The steady assembly of the outer kinetochore during the mitotic cell cycle diminishes the need for Nup132. This idea is also supported by the fact that mitotic delays were observed when hNup133 was depleted from the kinetochores in human cells (Zuccolo et al., 2007) as the human outer kinetochore is dynamically assembled and disassembled during mitosis (Gascoigne and Cheeseman, 2011). Because delays in the metaphase-anaphase transition occur in both human mitosis and *S. pombe* meiosis in the absence of hNup133/Nup132, human hNup133 and *S. pombe* Nup132 may play a similar, conserved role.

Materials and methods

Yeast strains and culture

The *S. pombe* strains used in this study are listed in Table S1. The culture media used here have been described previously (Moreno et al., 1991). All strains were grown on yeast extract with supplements (YES) plates or Edinburgh minimal medium (EMM) with the appropriate supplements at 30°C. Sporulation was induced on malt extract (ME) plates at 26°C. To induce meiosis entry, cells were freshly inoculated on a YES plate and were resuspended in nitrogen-free minimal medium supplemented with adenine, uracil, histidine, lysine, and leucine (EMM-N+5S) at a density of 10^9 cells/ml. The cell suspension was then spotted onto an ME plate. Heterothallic strains were premixed with EMM-N+5S medium before plating on the ME plate. After 8–10 h of incubation on the ME plates, the cells that had undergone karyogamy were selected for live-cell imaging. The sporulation frequency was determined after the cells were sporulated for 2 d on the ME plates.

The *nup132*$^+$ gene was disrupted with the *ura4*$^+$ gene by using the template plasmid of pCSU3 and the primers NM4-UPF (5′-ATGAAAAATAGCTTTCCGATTCGGC-3′), NM4-UPR (5′-CCCACAGTTCTAGAGGATCCGGTCAAGCTTAAACTACTTT-3′), NM4-DWF (5′-GCCTTAACGACGTAGTCGACTTTATCTTAATCATACAAAC-3′), and NM4-DWR (5′-CCGAGGCAGCCAACACTGTACTTGG-3′; Chikashige et al., 2006; Asakawa et al., 2014). The underlined portions are the sequences shared by the pCSU3 plasmid. In cases where the *ura4*$^+$ marker was not available, *nup132*$^+$ was deleted with a *kanMX6* marker or a *natMX6* marker (Krawchuk and Wahls, 1999; Hentges et al., 2005). The *nup132*$^+$ gene was disrupted with a drug resistance gene cassette (*kanMX6* or *natMX6*) by using pFA6a derivatives and the primers nup132D-1 (5′-GAAATCTGATGTTTCCAACC-3′), nup132D-R1 (5′-GAGGCAAGCTAAACAGATCTGACTATTTGACGATATCAGT-3′), nup132D-F2 (5′-GTTTAAACGAGCTCGAATTCTAACCTTTATCTTAATCATA-3′), and nup132D-2 (5′-GTTCATTACCGCGTTGG-3′). The underlined portions are the sequences shared by the pFA6a plasmid. The *nup132*$^+$ gene disruption was confirmed by PCR, and the phenotype of nontetrad formation or unevenly distributed nucleoporins (Baï et al., 2004; Asakawa et al., 2014). The *mad2*Δ background is derived from the HR105 strain (a gift from T. Matsumoto, Kyoto University, Kyoto, Japan; Kim et al., 1998), whereas the *bub1*Δ background is originated from strain 393 (a gift from J.-P. Javerzat, Institut de Biochimie et Génétique Cellulaires, Bordeaux, France; Bernard et al., 1998). The *rec12*Δ background was derived from the YY290-7B strain, in which the whole ORF of *rec12*$^+$ was replaced with the *kanMX6* marker (Ding et al., 2004). The *sgo1*Δ background originated from strain PZ856 (obtained from the Yeast Genetic Resource Center of Japan supported by the National BioResource Project; Hauf et al., 2007).

Unless stated otherwise, a two-step PCR method was used to introduce a chromosomal CFP, GFP, or mCherry tag to produce fluorescently labeled proteins (Hayashi et al., 2009). To visualize tubulin, integrating plasmids carrying GFP-*atb2*$^+$or mCherry-*atb2*$^+$ were introduced into the cells (Masuda et al., 2006; Unsworth et al., 2008). The telomere marker and nuclear reporter were encoded by plasmid-borne *taz1*$^+$-GFP and 3GFP-NLS integrated at the *lys1*$^+$-locus, respectively (Chikashige et al., 2006; Asakawa et al., 2010). mCherry-tagged histone H2B is expressed from an *aur1*^{r}-integrating plasmid that carries the mCherry-*htb1*$^+$ gene (Ruan et al., 2015). The *aur1*^{r} gene confers resistance to the toxic drug aureobasidin A (Takara Bio Inc.). To visualize the centromere of chromosome II, cells were crossed to strains carrying lacI-GFP and tandem repeats of the *lacO* sequence integrated at the *cen2*-proximal locus (Yamamoto and Hiraoka, 2003). Cells carrying GFP-3pk-*moa1*$^+$ are cross products derived from strain PZ425 (*GFP-3pk-moa1+-kanr, ade6-M216, leu1*; a gift from Y. Watanabe, University of Tokyo, Tokyo, Japan). The strains carrying *sgo1*$^+$*-flag-GFP* originated from strain FY13800 (*leu1 sgo1*$^+$*-flag-GFP ade6-M210 pREP81* [*CFP-atb2*+]), which was obtained from the Yeast Genetic Resource Center of Japan supported by the National BioResource Project. The Rhp51-ECFP strains are derived from strain YA1083 (TH805 *rhp51-ECFP::ura4+::rhp51*; a gift from H. Iwasaki, Tokyo Institute of Technology, Tokyo, Japan; Akamatsu et al., 2007).

Fluorescence microscopy

For the live-cell imaging, induced meiotic cells in the liquid medium of EMM-N+5S were immobilized on lectin (0.2 mg/ml; Sigma)–coated 35-mm glass-bottomed culture dishes (MatTek Corp.) and observed at 26°C (Asakawa and Hiraoka, 2009). Images were obtained with a DeltaVision deconvolution microscope system (Applied Precision, Inc.), in which an Olympus inverted microscope IX70 is equipped with an interline CoolSNAP HQ^2 charge-coupled device (Photometrics). The acquisition software was DeltaVision softWoRx 5.5. At each time point, optical section images were acquired at 0.3-µm or 0.5-µm intervals by using an Olympus oil-immersion 60× objective lens (PlanApoN60x OSC; NA = 1.4). Three-dimensional constrained iterative deconvolution of the images was done by the "enhanced ratio" method in softWoRx 5.5, and the images of Figs. 5, 6, 7, and 8 were processed using the denoising algorithm (Boulanger et al., 2009) before deconvolution.

Random spore assay

Cells were sporulated on ME plates for 3 d at 26°C. To release the spores, the asci were collected from the plate, suspended in a solution containing a 1:10 dilution of β-glucuronidase (Sigma), and incubated for several hours at 30°C. Breakdown of the ascus cell wall by the enzyme and spore release were verified under the microscope. Spore numbers were determined with a CDA-1000 particle analyzer (Sysmex Corp.), and the spores were properly diluted to spread on YES plates. The YES plates were incubated at 30°C for 3–4 d to allow for colony formation. Spore viability = number of colonies formed × dilution factor/total number of spores applied.

Online supplemental material

Fig. S1 shows additional evidence of the delays in the metaphase-anaphase transition in the *nup132*Δ mutant by tracking Cut2-GFP dynamics. Fig. S2 shows localization of 3GFP-NLS during meiosis. Fig. S3 shows centromere localization of Moa1-GFP and Sgo1-Flag-GFP during metaphase I in the *nup132*Δ mutant. Fig. S4 summarizes the timing at which the Mis12-GFP first appeared during meiotic prophase in the various mutants. Fig. S5 shows live-cell imaging of a wild-type cell expressing Csi1-mCherry during meiotic prophase. Table S1 lists the strain used in this study. Online supplemental material is available at http://www.jcb.org/cgi/content/full/jcb.201501035/DC1.

Acknowledgments

We are indebted to Yuji Chikashige and Atsushi Matsuda for valuable suggestions on image acquisition and processing. We thank Chizuru Ohtsuki, Kun Ruan, and Xu Zhang for technical assistance. We also thank Hiroshi Iwasaki, Jean-Paul Javerzat, Tomohiro Matsumoto, Yoshinori Watanabe, and the National BioResource Project for kindly providing yeast strains.

This work was supported by a Japan Society for the Promotion of Science postdoctoral fellowship to H.-J. Yang and by Ministry of Education, Cultutre, Sports, Science and Technology/Japan Society for the Promotion of Science KAKENHI grants to H. Asakawa, T. Haraguchi, and Y. Hiraoka.

The authors declare no competing financial interests.

Submitted: 9 January 2015
Accepted: 11 September 2015

References

Akamatsu, Y., Y. Tsutsui, T. Morishita, M.S.P. Siddique, Y. Kurokawa, M. Ikeguchi, F. Yamao, B. Arcangioli, and H. Iwasaki. 2007. Fission yeast Swi5/Sfr1 and Rhp55/Rhp57 differentially regulate Rhp51-dependent recombination outcomes. *EMBO J.* 26:1352–1362. http://dx.doi.org/10.1038/sj.emboj.7601582

Asakawa, H., and Y. Hiraoka. 2009. Live-cell fluorescence imaging of meiotic chromosome dynamics in *Schizosaccharomyces pombe*. *Methods Mol. Biol.* 558:53–64. http://dx.doi.org/10.1007/978-1-60761-103-5_4

Asakawa, H., A. Hayashi, T. Haraguchi, and Y. Hiraoka. 2005. Dissociation of the Nuf2-Ndc80 complex releases centromeres from the spindle-pole body during meiotic prophase in fission yeast. *Mol. Biol. Cell.* 16:2325–2338. http://dx.doi.org/10.1091/mbc.E04-11-0996

Asakawa, H., T. Haraguchi, and Y. Hiraoka. 2007. Reconstruction of the kinetochore: a prelude to meiosis. *Cell Div.* 2:17. http://dx.doi.org/10.1186/1747-1028-2-17

Asakawa, H., T. Kojidani, C. Mori, H. Osakada, M. Sato, D.-Q. Ding, Y. Hiraoka, and T. Haraguchi. 2010. Virtual breakdown of the nuclear envelope in fission yeast meiosis. *Curr. Biol.* 20:1919–1925. http://dx.doi.org/10.1016/j.cub.2010.09.070

Asakawa, H., H.-J. Yang, T.G. Yamamoto, C. Ohtsuki, Y. Chikashige, K. Sakata-Sogawa, M. Tokunaga, M. Iwamoto, Y. Hiraoka, and T. Haraguchi. 2014. Characterization of nuclear pore complex components in fission yeast *Schizosaccharomyces pombe*. *Nucleus.* 5:149–162. http://dx.doi.org/10.4161/nucl.28487

Baï, S.W., J. Rouquette, M. Umeda, W. Faigle, D. Loew, S. Sazer, and V. Doye. 2004. The fission yeast Nup107-120 complex functionally interacts with the small GTPase Ran/Spi1 and is required for mRNA export, nuclear pore distribution, and proper cell division. *Mol. Cell. Biol.* 24:6379–6392. http://dx.doi.org/10.1128/MCB.24.14.6379-6392.2004

Belgareh, N., G. Rabut, S.W. Baï, M. van Overbeek, J. Beaudouin, N. Daigle, O.V. Zatsepina, F. Pasteau, V. Labas, M. Fromont-Racine, et al. 2001. An evolutionarily conserved NPC subcomplex, which redistributes in part to kinetochores in mammalian cells. *J. Cell Biol.* 154:1147–1160. http://dx.doi.org/10.1083/jcb.200101081

Bernard, P., K. Hardwick, and J.P. Javerzat. 1998. Fission yeast bub1 is a mitotic centromere protein essential for the spindle checkpoint and the preservation of correct ploidy through mitosis. *J. Cell Biol.* 143:1775–1787. http://dx.doi.org/10.1083/jcb.143.7.1775

Bernard, P., J.F. Maure, and J.P. Javerzat. 2001. Fission yeast Bub1 is essential in setting up the meiotic pattern of chromosome segregation. *Nat. Cell Biol.* 3:522–526. http://dx.doi.org/10.1038/35074598

Bolhy, S., I. Bouhlel, E. Dultz, T. Nayak, M. Zuccolo, X. Gatti, R. Vallee, J. Ellenberg, and V. Doye. 2011. A Nup133-dependent NPC-anchored network tethers centrosomes to the nuclear envelope in prophase. *J. Cell Biol.* 192:855–871. http://dx.doi.org/10.1083/jcb.201007118

Boratyn, G.M., A.A. Schäffer, R. Agarwala, S.F. Altschul, D.J. Lipman, and T.L. Madden. 2012. Domain enhanced lookup time accelerated BLAST. *Biol. Direct.* 7:12. http://dx.doi.org/10.1186/1745-6150-7-12

Boulanger, J., C. Kervrann, and P. Bouthemy. 2009. A simulation and estimation framework for intracellular dynamics and trafficking in video-microscopy and fluorescence imagery. *Med. Image Anal.* 13:132–142. http://dx.doi.org/10.1016/j.media.2008.06.017

Cheeseman, I.M., J.S. Chappie, E.M. Wilson-Kubalek, and A. Desai. 2006. The conserved KMN network constitutes the core microtubule-binding site of the kinetochore. *Cell.* 127:983–997. http://dx.doi.org/10.1016/j.cell.2006.09.039

Chikashige, Y., D.Q. Ding, H. Funabiki, T. Haraguchi, S. Mashiko, M. Yanagida, and Y. Hiraoka. 1994. Telomere-led premeiotic chromosome movement in fission yeast. *Science.* 264:270–273. http://dx.doi.org/10.1126/science.8146661

Chikashige, Y., D.Q.D. Ding, Y. Imai, M. Yamamoto, T. Haraguchi, and Y. Hiraoka. 1997. Meiotic nuclear reorganization: switching the position of centromeres and telomeres in the fission yeast *Schizosaccharomyces pombe*. *EMBO J.* 16:193–202. http://dx.doi.org/10.1093/emboj/16.1.193

Chikashige, Y., R. Kurokawa, T. Haraguchi, and Y. Hiraoka. 2004. Meiosis induced by inactivation of Pat1 kinase proceeds with aberrant nuclear positioning of centromeres in the fission yeast Schizosaccharomyces pombe. *Genes Cells.* 9:671–684. http://dx.doi.org/10.1111/j.1356-9597.2004.00760.x

Chikashige, Y., C. Tsutsumi, M. Yamane, K. Okamasa, T. Haraguchi, and Y. Hiraoka. 2006. Meiotic proteins bqt1 and bqt2 tether telomeres to form the bouquet arrangement of chromosomes. *Cell.* 125:59–69. http://dx.doi.org/10.1016/j.cell.2006.01.048

Davis, L., and G.R.G. Smith. 2003. Nonrandom homolog segregation at meiosis I in *Schizosaccharomyces pombe* mutants lacking recombination. *Genetics.* 163:857–874.

Desai, A., S. Rybina, T. Müller-Reichert, A. Shevchenko, A. Shevchenko, A. Hyman, and K. Oegema. 2003. KNL-1 directs assembly of the microtubule-binding interface of the kinetochore in C. elegans. *Genes Dev.* 17:2421–2435. http://dx.doi.org/10.1101/gad.1126303

Ding, D.-Q., A. Yamamoto, T. Haraguchi, and Y. Hiraoka. 2004. Dynamics of homologous chromosome pairing during meiotic prophase in fission yeast. *Dev. Cell.* 6:329–341. http://dx.doi.org/10.1016/S1534-5807(04)00059-0

Ding, D.-Q., N. Sakurai, Y. Katou, T. Itoh, K. Shirahige, T. Haraguchi, and Y. Hiraoka. 2006. Meiotic cohesins modulate chromosome compaction during meiotic prophase in fission yeast. *J. Cell Biol.* 174:499–508.

Espeut, J., D.K. Cheerambathur, L. Krenning, K. Oegema, and A. Desai. 2012. Microtubule binding by KNL-1 contributes to spindle checkpoint silencing at the kinetochore. *J. Cell Biol.* 196:469–482. http://dx.doi.org/10.1083/jcb.201111107

Funabiki, H., H. Yamano, K. Kumada, K. Nagao, T. Hunt, and M. Yanagida. 1996. Cut2 proteolysis required for sister-chromatid separation in fission yeast. *Nature.* 381:438–441. http://dx.doi.org/10.1038/381438a0

Gascoigne, K.E., and I.M. Cheeseman. 2011. Kinetochore assembly: if you build it, they will come. *Curr. Opin. Cell Biol.* 23:102–108. http://dx.doi.org/10.1016/j.ceb.2010.07.007

Hauf, S., and Y. Watanabe. 2004. Kinetochore orientation in mitosis and meiosis. *Cell.* 119:317–327. http://dx.doi.org/10.1016/j.cell.2004.10.014

Hauf, S., A. Biswas, M. Langegger, S.A.S. Kawashima, T. Tsukahara, and Y. Watanabe. 2007. Aurora controls sister kinetochore mono-orientation and homolog bi-orientation in meiosis-I. *EMBO J.* 26:4475–4486. http://dx.doi.org/10.1038/sj.emboj.7601880

Hayashi, A., H. Asakawa, T. Haraguchi, and Y. Hiraoka. 2006. Reconstruction of the kinetochore during meiosis in fission yeast *Schizosaccharomyces pombe*. *Mol. Biol. Cell.* 17:5173–5184. http://dx.doi.org/10.1091/mbc.E06-05-0388

Hayashi, A., D.Q. Ding, C. Tsutsumi, Y. Chikashige, H. Masuda, T. Haraguchi, and Y. Hiraoka. 2009. Localization of gene products using a chromosomally tagged GFP-fusion library in the fission yeast *Schizosaccharomyces pombe*. *Genes Cells.* 14:217–225. http://dx.doi.org/10.1111/j.1365-2443.2008.01264.x

Hentges, P., B. Van Driessche, L. Tafforeau, J. Vandenhaute, and A.M. Carr. 2005. Three novel antibiotic marker cassettes for gene disruption and marker switching in *Schizosaccharomyces pombe*. *Yeast.* 22:1013–1019. http://dx.doi.org/10.1002/yea.1291

Hirose, Y., R. Suzuki, T. Ohba, Y. Hinohara, H. Matsuhara, M. Yoshida, Y. Itabashi, H. Murakami, and A. Yamamoto. 2011. Chiasmata promote monopolar attachment of sister chromatids and their co-segregation toward the proper pole during meiosis I. *PLoS Genet.* 7:e1001329. http://dx.doi.org/10.1371/journal.pgen.1001329

Hou, H., Z. Zhou, Y. Wang, J. Wang, S.P.S. Kallgren, T. Kurchuk, E.A.E. Miller, F. Chang, and S. Jia. 2012. Csi1 links centromeres to the nuclear envelope for centromere clustering. *J. Cell Biol.* 199:735–744. http://dx.doi.org/10.1083/jcb.201208001

Kim, S.H.S., D.P.D. Lin, S. Matsumoto, A. Kitazono, and T. Matsumoto. 1998. Fission yeast Slp1: an effector of the Mad2-dependent spindle checkpoint. *Science.* 279:1045–1047. http://dx.doi.org/10.1126/science.279.5353.1045

Kitajima, T.S., S.A. Kawashima, and Y. Watanabe. 2004. The conserved kinetochore protein shugoshin protects centromeric cohesion during meiosis. *Nature.* 427:510–517. http://dx.doi.org/10.1038/nature02312

Kitajima, T.S.T., Y. Miyazaki, M. Yamamoto, and Y. Watanabe. 2003. Rec8 cleavage by separase is required for meiotic nuclear divisions in fission yeast. *EMBO J.* 22:5643–5653. http://dx.doi.org/10.1093/emboj/cdg527

Krawchuk, M.D., and W.P. Wahls. 1999. High-efficiency gene targeting in *Schizosaccharomyces pombe* using a modular, PCR-based approach with long tracts of flanking homology. *Yeast.* 15:1419–1427. http://dx.doi.org/10.1002/(SICI)1097-0061(19990930)15:13<1419::AID-YEA466>3.0.CO;2-Q

Masuda, H., R. Miyamoto, T. Haraguchi, and Y. Hiraoka. 2006. The carboxy-terminus of Alp4 alters microtubule dynamics to induce oscillatory nuclear movement led by the spindle pole body in *Schizosaccharomyces pombe*. *Genes Cells.* 11:337–352. http://dx.doi.org/10.1111/j.1365-2443.2006.00947.x

Mishra, R.K., P. Chakraborty, A. Arnaoutov, B.M.A. Fontoura, and M. Dasso. 2010. The Nup107-160 complex and gamma-TuRC regulate microtubule polymerization at kinetochores. *Nat. Cell Biol.* 12:164–169. http://dx.doi.org/10.1038/ncb2016

Molnar, M., J. Bähler, J. Kohli, and Y. Hiraoka. 2001a. Live observation of fission yeast meiosis in recombination-deficient mutants: a study on achiasmate chromosome segregation. *J. Cell Sci.* 114:2843–2853.

Molnar, M., S. Parisi, Y. Kakihara, H. Nojima, A. Yamamoto, Y. Hiraoka, A. Bozsik, M. Sipiczki, and J. Kohli. 2001b. Characterization of rec7, an early meiotic recombination gene in *Schizosaccharomyces pombe*. *Genetics.* 157:519–532.

Moreno, S., A. Klar, and P. Nurse. 1991. Molecular genetic analysis of fission yeast *Schizosaccharomyces pombe*. *Methods Enzymol.* 194:795–823. http://dx.doi.org/10.1016/0076-6879(91)94059-L

Nabeshima, K., T. Nakagawa, A.F.A. Straight, A. Murray, Y. Chikashige, Y.M.Y. Yamashita, Y. Hiraoka, and M. Yanagida. 1998. Dynamics of centromeres during metaphase-anaphase transition in fission yeast: Dis1 is implicated in force balance in metaphase bipolar spindle. *Mol. Biol. Cell.* 9:3211–3225. http://dx.doi.org/10.1091/mbc.9.11.3211

Ohta, M., M. Sato, and M. Yamamoto. 2012. Spindle pole body components are reorganized during fission yeast meiosis. *Mol. Biol. Cell.* 23:1799–1811. http://dx.doi.org/10.1091/mbc.E11-11-0951

Parra, M.T., A. Viera, R. Gómez, J. Page, R. Benavente, J.L. Santos, J.S. Rufas, and J.A. Suja. 2004. Involvement of the cohesin Rad21 and SCP3 in monopolar attachment of sister kinetochores during mouse meiosis I. *J. Cell Sci.* 117:1221–1234. http://dx.doi.org/10.1242/jcs.00947

Przewloka, M.R., Z. Venkei, V.M. Bolanos-Garcia, J. Debski, M. Dadlez, and D.M. Glover. 2011. CENP-C is a structural platform for kinetochore assembly. *Curr. Biol.* 21:399–405. http://dx.doi.org/10.1016/j.cub.2011.02.005

Rago, F., and I.M. Cheeseman. 2013. Review series: the functions and consequences of force at kinetochores. *J. Cell Biol.* 200:557–565. http://dx.doi.org/10.1083/jcb.201211113

Ródenas, E., C. González-Aguilera, C. Ayuso, and P. Askjaer. 2012. Dissection of the NUP107 nuclear pore subcomplex reveals a novel interaction with spindle assembly checkpoint protein MAD1 in *Caenorhabditis elegans*. *Mol. Biol. Cell.* 23:930–944. http://dx.doi.org/10.1091/mbc.E11-11-0927

Ruan, K., T.G. Yamamoto, H. Asakawa, Y. Chikashige, H. Masukata, T. Haraguchi, and Y. Hiraoka. 2015. Meiotic nuclear movements in fission yeast are regulated by the transcription factor Mei4 downstream of a Cds1-dependent replication checkpoint pathway. *Genes Cells* 20:160–172.

Screpanti, E., A. De Antoni, G.M. Alushin, A. Petrovic, T. Melis, E. Nogales, and A. Musacchio. 2011. Direct binding of Cenp-C to the Mis12 complex joins the inner and outer kinetochore. *Curr. Biol.* 21:391–398. http://dx.doi.org/10.1016/j.cub.2010.12.039

Shepperd, L.A., J.C. Meadows, A.M. Sochaj, T.C. Lancaster, J. Zou, G.J. Buttrick, J. Rappsilber, K.G. Hardwick, and J.B.A. Millar. 2012. Phosphodependent recruitment of Bub1 and Bub3 to Spc7/KNL1 by Mph1 kinase maintains the spindle checkpoint. *Curr. Biol.* 22:891–899. http://dx.doi.org/10.1016/j.cub.2012.03.051

Uchida, K.S.K., K. Takagaki, K. Kumada, Y. Hirayama, T. Noda, and T. Hirota. 2009. Kinetochore stretching inactivates the spindle assembly checkpoint. *J. Cell Biol.* 184:383–390. http://dx.doi.org/10.1083/jcb.200811028

Unsworth, A., H. Masuda, S. Dhut, and T. Toda. 2008. Fission yeast kinesin-8 Klp5 and Klp6 are interdependent for mitotic nuclear retention and required for proper microtubule dynamics. *Mol. Biol. Cell.* 19:5104–5115. http://dx.doi.org/10.1091/mbc.E08-02-0224

Watanabe, Y., and P. Nurse. 1999. Cohesin Rec8 is required for reductional chromosome segregation at meiosis. *Nature.* 400:461–464. http://dx.doi.org/10.1038/22774

West, R.R., E.V. Vaisberg, R. Ding, P. Nurse, and J.R. McIntosh. 1998. cut11^{+}: A gene required for cell cycle-dependent spindle pole body anchoring in the nuclear envelope and bipolar spindle formation in *Schizosaccharomyces pombe*. *Mol. Biol. Cell.* 9:2839–2855. http://dx.doi.org/10.1091/mbc.9.10.2839

Yamamoto, A., and Y. Hiraoka. 2003. Monopolar spindle attachment of sister chromatids is ensured by two distinct mechanisms at the first meiotic division in fission yeast. *EMBO J.* 22:2284–2296. http://dx.doi.org/10.1093/emboj/cdg222

Yamamoto, A., K. Kitamura, D. Hihara, Y. Hirose, S. Katsuyama, and Y. Hiraoka. 2008. Spindle checkpoint activation at meiosis I advances anaphase II onset via meiosis-specific APC/C regulation. *J. Cell Biol.* 182:277–288. http://dx.doi.org/10.1083/jcb.200802053

Yokobayashi, S., and Y. Watanabe. 2005. The kinetochore protein Moa1 enables cohesion-mediated monopolar attachment at meiosis I. *Cell.* 123:803–817. http://dx.doi.org/10.1016/j.cell.2005.09.013

Zimmerman, S., R.R. Daga, and F. Chang. 2004. Intra-nuclear microtubules and a mitotic spindle orientation checkpoint. *Nat. Cell Biol.* 6:1245–1246. http://dx.doi.org/10.1038/ncb1200

Zuccolo, M., A. Alves, V. Galy, S. Bolhy, E. Formstecher, V. Racine, J.-B. Sibarita, T. Fukagawa, R. Shiekhattar, T. Yen, and V. Doye. 2007. The human Nup107-160 nuclear pore subcomplex contributes to proper kinetochore functions. *EMBO J.* 26:1853–1864. http://dx.doi.org/10.1038/sj.emboj.7601642